Advances in Theoretical and Applied Mechanics, Vol. 10, 2017, no. 1, 11 - 20
HIKARI Ltd, www.m-hikari.com
https://doi.org/10.12988/atam.2017.752

Analysis of Fluid Dynamics and Heat Transfer inside an Elliptical Cylinder in a Square Enclosure

Marhama Jelita, Halim Mudia and Susi Afriani

Department of Electrical Engineering
Faculty of Science Technology
Universitas Islam Sultan Syarif Kasim (UIN Suska)
28293 Pekanbaru, Riau, Indonesia

Abstract

The present study investigates the natural convection induced by a temperature difference between a cold outer square enclosure and a hot inner elliptical cylinder. The governing equations are solved numerically using the built-in finite element method of COMSOL. The governing parameters considered are the major and minor axis lengths, the orientation angle and the Rayleigh number. It is found that the convective flow depends on the Rayleigh number, elliptical shape and orientation.

Subject Classification: 76S05

Keywords: fluid dynamics, natural convection, cold enclosure, hot elliptical cylinder

1 Introduction

Fluid dynamics and convection heat transfer from a heated body inside enclosures has long been studied and has received more attention due to its direct

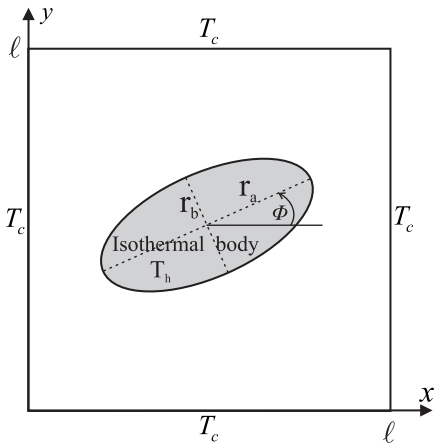

Figure 1: Schematic representation of the model

relevancy to many engineering and technological applications. Natural convection in enclosures containing a heated circular cylinder is studied rigorously in the literature. N.K. Ghaddar [1] found that the maximum air velocity was at a distance of about nine cylinder diameters along the vertical centerline above the heated cylinder. F. Moukalled and S. Acharya [2] analyzed the effect of the radius of the inner circular cylinder and the aspect ratio to the convective flow. The heat transfer enhancement by increasing the cylinder size and/or surface emissivity was obtained by A. Mezrhab et al. [3]. B.S. Kim et al. [4] showed the cylinder position could affect heat transfer quantities. Effect of horizontal and vertical equal distance of inner cylinders was investigated in [5].

Comparatively, fewer publications were found for natural convection in an enclosure containing a heated non-circular cylinder, such as elliptical cylinder. Elliptical geometries have an excellence of performance compared to circular geometries in many industrial applications, where heat loads are substantial and space is limited, require the use of tubular heat exchangers for the cooling of electronic equipment. Elliptical cylinders offer less flow resistance and higher heat-transfer rates than circular cylinders as reported by [6, 7]. They provide more general geometrical configurations than circular cylinders. Therefore, the aim of present work is to investigate numerically the problem of natural convection from a heated elliptical cylinder embedded in a cold square enclosure. The flow fields, temperature distributions and the heat transfer rate will be presented graphically.

2 Mathematical Formulation

A schematic diagram of a cold square enclosure having an inner hot elliptical cylinder is shown in Fig. 1. The elliptical cylinder is located in the center of enclosure with major axis $2r_a$ and minor axis $2r_b$. The orientation angle ϕ which is the inclination angle of the major axis of the heated elliptical cylinder to the horizontal direction. Under the influence of the vertical gravitational field, the elliptical cylinder and walls at different levels of temperature lead to a natural convection problem. The governing equations are transformed into dimensionless form under the following non-dimensional variables

$$X = \frac{x}{\ell},\ Y = \frac{y}{\ell},\ U = \frac{u\ell}{\alpha},\ V = \frac{v\ell}{\alpha}, \Theta = \frac{T - T_c}{T_h - T_c}, \quad R_a = \frac{r_a}{\ell}, \tag{1}$$
$$R_b = \frac{r_b}{\ell},\ Pr = \frac{\nu}{\alpha},\ Ra = \frac{g\beta\left(T_h - T_c\right)\ell^3}{\nu\alpha},\ P = \frac{p\ell^2}{\rho\alpha}$$

The dimensionless form of the governing equations are expressed as follows:

$$\frac{\partial U}{\partial X} + \frac{\partial V}{\partial Y} = 0 \tag{2}$$
$$U\frac{\partial U}{\partial X} + V\frac{\partial U}{\partial Y} = -\frac{\partial P}{\partial X} + Pr\left(\frac{\partial^2 U}{\partial X^2} + \frac{\partial^2 U}{\partial Y^2}\right) \tag{3}$$
$$U\frac{\partial V}{\partial X} + V\frac{\partial V}{\partial Y} = -\frac{\partial P}{\partial X}Pr\left(\frac{\partial^2 V}{\partial X^2} + \frac{\partial^2 V}{\partial Y^2}\right) + Ra\,Pr\,\Theta \tag{4}$$
$$U\frac{\partial \Theta}{\partial X} + V\frac{\partial \Theta}{\partial Y} = \left(\frac{\partial^2 \Theta}{\partial X^2} + \frac{\partial^2 \Theta}{\partial Y^2}\right) \tag{5}$$

$U = V = 0$ on the walls of the enclosure and elliptical cylinder. The boundary conditions for the non-dimensional temperatures are:

$$\begin{array}{ll} \text{on outer walls} & \Theta = 0 \\ \text{on elliptical cylinder} & \Theta = 1 \end{array} \tag{6}$$

Heat transfer rate is very important in thermal engineering applications. Therefore, the rate of heat transfer is computed at inner wall and is expressed in terms of local surface Nusselt number (Nu) and surface-averaged Nusselt number ($\overline{Nu}$) as:

$$Nu = \frac{\partial \Theta}{\partial n}\Big|_{\text{wall}}, \quad \overline{Nu} = \frac{1}{W}\int_0^W Nu\S \tag{7}$$

where n is the normal direction with respect to the wall, W is the surface area of the wall.

Table 1: Grid sensitivity check at $Ra = 10^5$ and $R_a = 0.2$, $R_b = 0.1$ and $\phi = 0°$.

Predefined mesh size	Mesh elements	$\Psi_{\min}$	$\Psi_{\max}$	$\overline{Nu}$	CPU time (s)
Extremely coarse	332	−5.1021	5.0525	3.4691	2
Extra coarse	494	−5.5017	5.6779	3.5251	2
Coarser	814	−6.0961	6.1068	3.6876	2
Coarse	1400	−6.6059	6.6184	3.7904	3
Normal	2032	−6.9560	7.0215	3.8688	3
Fine	3026	−7.3089	7.3164	3.9210	4
Finer	7732	−7.7707	7.7919	4.0079	8
Extra fine	20734	−8.2166	8.2129	4.1001	25
Extremely fine	27398	−8.4470	8.4500	4.1230	29

3 Computational Methodology

The governing equations along with the boundary condition are modelled and solved numerically by the COMSOL. COMSOL is a general-purpose solver of interlinked partial differential equation (PDE) based on the Galerkin finite element method (GFEM). This program contains state-of-the-art numerical algorithms and visualization tools bundled together with an easy to use interface. We consider the following application modes in COMSOL. The incompressible, laminar flow (spf) for Eqs. (2)–(4) and the heat transfer in fluids (ht) for Eq. (5).

Several grid sensitivity tests were conducted to determine the sufficiency of the mesh scheme and to ensure that the results are grid independent. We use the COMSOL default mesh settings, type physics-controlled mesh sizes, i.e. extremely coarse, extra coarse, coarser, coarse, normal, fine, finer, extra fine and extremely fine. In the tests, we consider the parameters $Ra = 10^5$ and $R_a = 0.2$, $R_b = 0.1$ and $\phi = 0°$ as tabulated in the Table 1. Considering both accuracy and time, a finer mesh size was selected for all the computations done in this paper.

4 Results and Discussion

The analysis in the undergoing numerical investigation are performed in the following domain of the associated dimensionless groups: the major axis length, $0.1 \leq R_a \leq 0.4$, the minor axis length, $0.05 \leq R_b \leq 0.20$, the orientation angle, $0° \leq \phi \leq 180°$ and the Rayleigh number, $10^3 \leq Ra \leq 10^7$. The working fluid

is taken as air and the Prandtl number is fixed at $Pr = 0.7$.

Fig. 2 illustrates the streamlines for various values of major axis length R_a while the Rayleigh number attains the value 10^3, 10^5 and 10^7, respectively. The minor axis length is fixed at $R_b = 0.15$ and the orientation angle is also fixed at $\phi = 0°$. The heated fluid adjoining the hot elliptical cylinder rises and moves upward due to buoyancy force. This movement is clearly seen from the Fig. 2(a) and it creates an anti-clockwise circulation cell in the left-half of the enclosure and clockwise circulation cell in the right-half of the enclosure. The streamline shows that two symmetrical flow circulations for all Rayleigh numbers at $R_a = 0.1$. Single eddy is found above the the inner elliptical cylinder for $Ra = 10^7$ at $0.1 \leq R_a \leq 0.3$ while at $R_a = 0.4$ the big cylinder breaks the single eddy into two eddies. The strength of the flow circulations decreases by increasing the major axis length. It is obvious that increasing the Rayleigh number increases the flow circulation. The flow below the hot cylinder, i.e., lower half of the cavity, is stagnant in the high values of Rayleigh number due to strong buoyancy force exists inside the enclosure. The core region of the symmetrical flow structure is split on increasing the major axis length R_a. When $R_a > 0.2$, multi-cellular flow structure is observed for low and moderate Rayleigh numbers while dual cellular flow structure is observed for high Rayleigh number.

Fig. 3 illustrates the streamlines for various values of orientation angle while the Rayleigh number attains the value 10^3, 10^5 and 10^7, respectively. The major and minor axis length are fixed at $R_a = 0.3$ and $R_b = 0.15$, respectively. The flow circulations are not symmetrical at $\phi = 45°$ and $\phi = 135°$. The flow pattern changes drastically on changing the values of $\phi = 135$. Firstly, the strength of the flow circulations increases by increasing the ϕ, but increasing the orientation angle further leads to decrease the strength of the flow circulations. The eddy on the left and right side in the flow expands in size by increasing the Rayleigh number at the fixed orientation angle. This is because the great buoyancy force is then happen when the Ra increases. It is interesting to note that two additional counter rotating eddies are found above the the inner elliptical cylinder for $Ra = 10^7$ at $\phi = 90°$. This fact is due to the great buoyancy force happen on the narrow space above the cylinder. Dual or multi-cellular structure is formed according to the values of ϕ. It clearly shows that the fluid dynamics are strongly depends on the orientation of elliptical cylinder (ϕ).

Variations of the surface-averaged average Nusselt number with the orientation angles are shown in Fig. 4 for various values of major and minor axis length at $Ra = 10^5$. The $\overline{Nu}$ has a minimum value at $\phi = 90°$ and small major axis length as shown in the top of Fig. 4. At very wide R_a, the effect of buoyancy-induced convection has different characteristic. The surface-averaged average Nusselt number has a local peak value at $\phi = 90°$

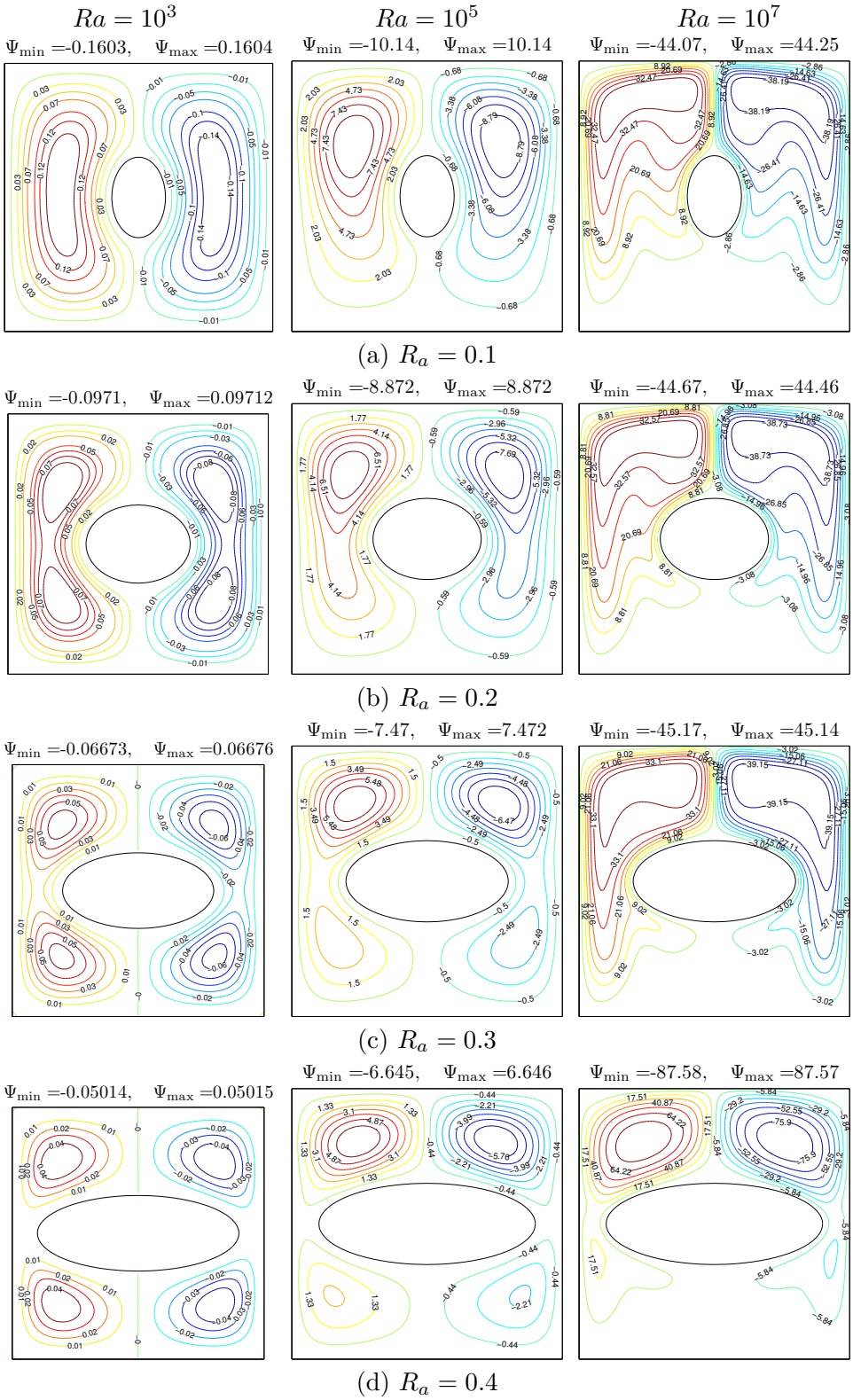

Figure 2: Streamlines for different Rayleigh numbers and major axis length R_a at minor axis length $R_b = 0.15$.

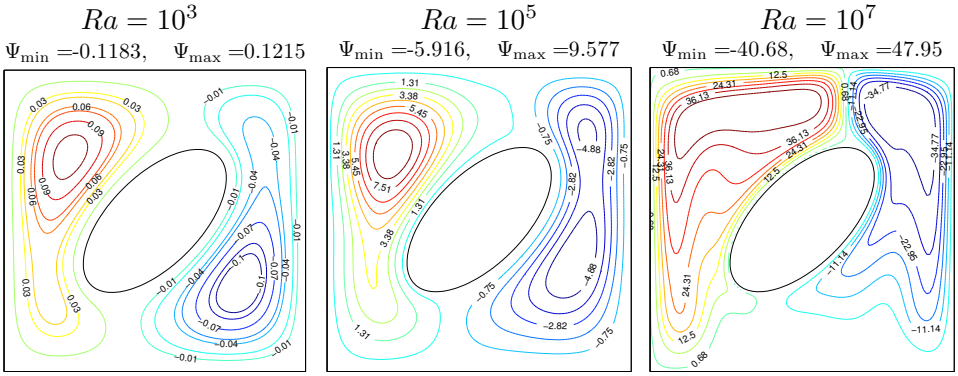

(a) $\phi = 45°$

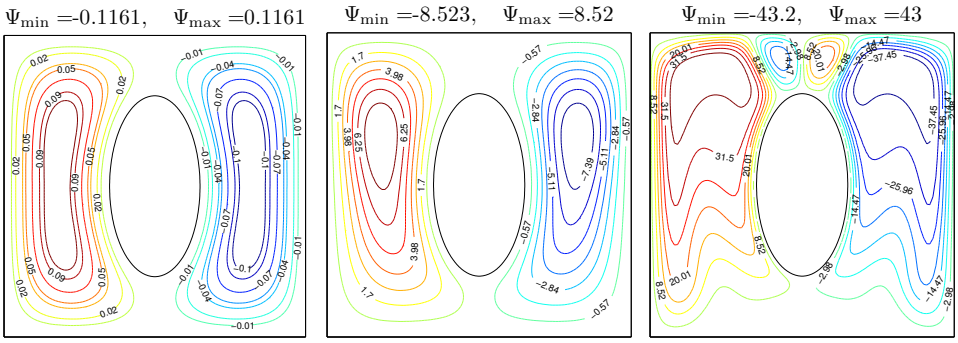

(b) $\phi = 90°$

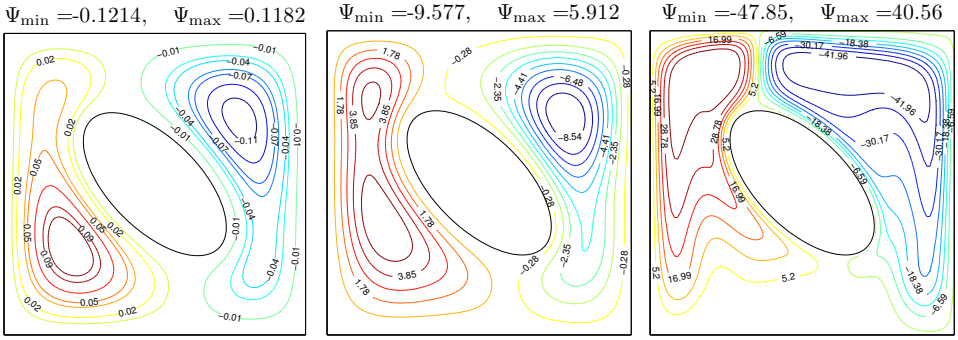

(c) $\phi = 135°$

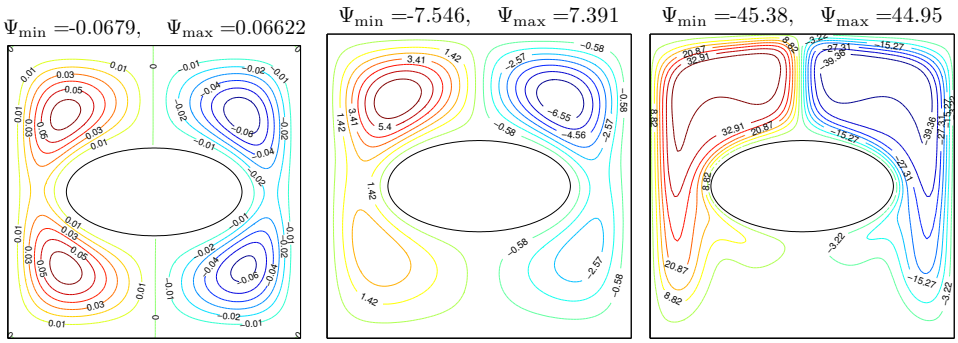

(d) $\phi = 180°$

Figure 3: Streamlines for different Rayleigh numbers and orientation angle ϕ at $R_a = 0.3$ and $R_b = 0.15$

and decreases with adjusted the ϕ up to 40° from the $\phi = 90°$. This situation also happen for the tall R_b as shown in the bottom of Fig. 4. The $\overline{Nu}$ has a local peak value at $\phi = 90°$ and decreases with adjusted the ϕ up to 50° to the left or to the right. Decreasing the minor axis length suppresses the peak and eventually at very thin elliptical cylinder ($R_b = 0.05$), the peak vanishes. When R_a is up to 0.3, the effect of R_a on heat transfer is little. However, the heat transfer is increased drastically at $R_a = 0.4$ and behaves non-linearly with orientation angle ϕ. At other values of R_a, ($R_a \leq 0.3$), heat transfer is decreased first up to $\phi = 90°$ then increased on increasing the values of ϕ. Heat transfer is decreased (increased) much at $0° \leq \phi \leq 45°$ (at $135° \leq \phi \leq 180°$) on increasing the orientation angle ϕ for different R_b values. Heat transfer is almost constant for given value of R_b in the range $45° \leq \phi \leq 135°$. The $\overline{Nu}$ profile by increasing the orientation angle of the major axis shows the symmetric distribution to the right angle of the major axis. Comparing the effects of R_a and R_b, R_a pronounces more on heat transfer.

5 Conclusions

The present numerical study investigates the natural convection induced by a temperature difference between a cold outer square enclosure and a hot inner elliptical cylinder. The dimensionless forms of the governing equations are modelled and solved using the built-in FEM of COMSOL Multiphysics software. The flow field depends on the elliptical shape, orientation and Rayleigh number. The heat transfer profile by increasing the orientation angle of the major axis shows the symmetric distribution to the right angle of the major axis. A local peak value of the heat transfer is also found at this orientation angle for a wide and tall elliptical cylinder.

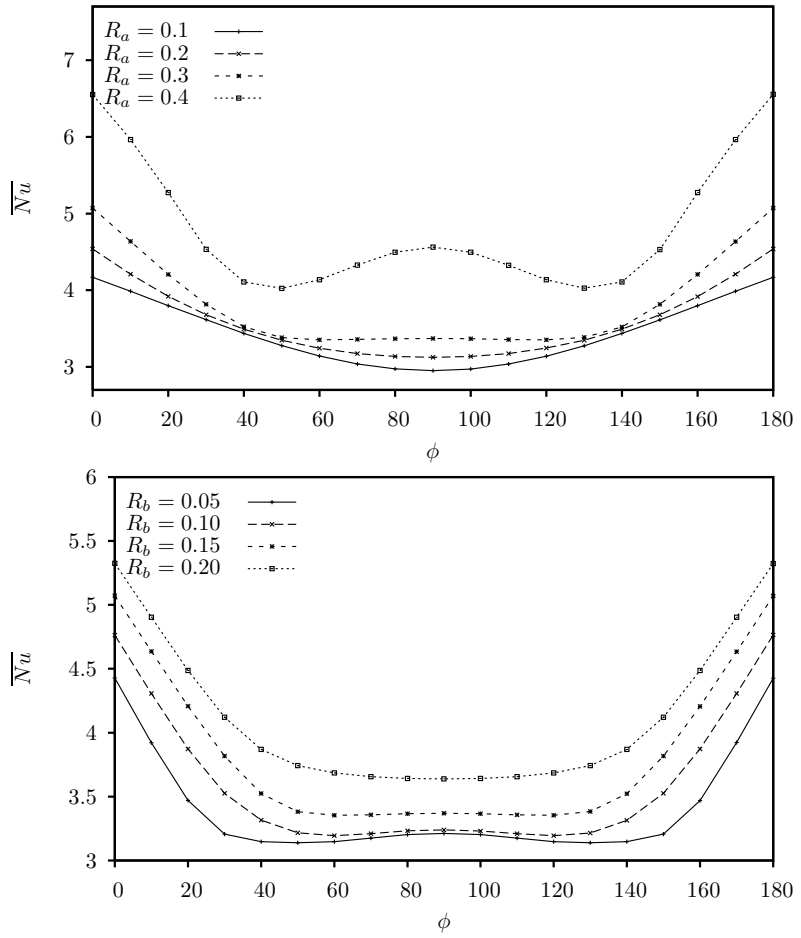

Figure 4: Surface-averaged Nusselt number $\overline{Nu}$ versus orientation angle for various value of R_a and R_b at $Ra = 10^5$.

References

[1] N.K. Ghaddar, Natural convection heat transfer between a uniformly heated cylindrical element and its rectangular enclosure, *Int. J. Heat Mass Transf.*, **35** (1992), 2327–2334. https://doi.org/10.1016/0017-9310(92)90075-4

[2] F. Moukalled and S. Acharya, Natural convection in the annulus between concentric horizontal circular and square cylinders, *J. Thermophys. Heat Transf.*, **10** (1996), 524–531. https://doi.org/10.2514/3.820

[3] A. Mezrhab, M. A. Moussaoui and H. Naji, Lattice Boltzmann simulation of surface radiation and natural convection in a square cavity with an inner cylinder, *Journal of Physics D: Applied Physics*, **41** (2008), no. 11, 115502. https://doi.org/10.1088/0022-3727/41/11/115502

[4] B.S. Kim, D.S. Lee, M.Y. Ha and H.S. Yoon, A numerical study of natural convection in a square enclosure with a circular cylinder at different vertical locations, *Int. J. Heat Mass Transf.*, **51** (2008), 1888–1906. https://doi.org/10.1016/j.ijheatmasstransfer.2007.06.033

[5] Gi Su Mun, Yong Gap Park, Hyun Sik Yoon, Minsung Kim and Man Yeong Ha, Natural convection in a cold enclosure with four hot inner cylinders based on diamond arrays (part-i: Effect of horizontal and vertical equal distance of inner cylinders), *International Journal of Heat and Mass Transfer*, **111** (2017), 755–770. https://doi.org/10.1016/j.ijheatmasstransfer.2017.04.004

[6] Y.D. Zhu, C. Shu, J. Qiu and J. Tani, Numerical simulation of natural convection between two elliptical cylinders using DQ method, *Int. J. Heat Mass Transf.*, **47** (2004), 797–808. https://doi.org/10.1016/j.ijheatmasstransfer.2003.06.005

[7] H.K. Dawood, H.A. Mohammed and K.M. Munisamy, Heat transfer ugmentation using nanofluids in an elliptic annulus with constant heat flux boundary condition, *Case Studies in Thermal Engineering*, **4** (2014), 32–41. https://doi.org/10.1016/j.csite.2014.06.001

Received: May 23, 2017; Published: July 25, 2017